

Supplement 1

METHODS AND MATERIALS

PET Acquisition and Reconstruction

[¹¹C]MDL100907 was prepared from desmethyl MDL100907 and [¹¹C]methyl triflate according to a modified procedure from Lundkvist, *et al* (S1). All scanning was performed on the ECAT EXACT HR+ scanner in 3D mode (Siemens/CTI, Knoxville, TN). Following a 15-minute transmission scan for attenuation correction, [¹¹C]MDL100907 was injected i.v. as a single bolus over 30 seconds. Emission data were acquired for 90 minutes for most participants (i.e., all patients and 16 of the 25 controls). However, 8 of the control participants received a 150-minute emission scan and 1 control underwent emission scanning for 120 minutes. To make the data for these subjects comparable to that of the rest of the sample, only the data acquired for the first 90 minutes were used for this subset of controls. Emission data were acquired as frames of increasing duration (3 * 20 s, 3 * 1 min, 3 * 2 min, 2 * 5 min, 7 * 10 min). After attenuation correction, data were reconstructed by filtered backprojection with a Shepp filter (cutoff 0.5 cycles/projection ray).

Following radiotracer injection, arterial samples were collected to form an input function for kinetic modeling. Samples were collected with an automated sampling system for the first 4 minutes (at 10-second intervals for the first 2 minutes and 20-second intervals for the following 2 minutes), and manually thereafter at longer intervals. A total of 29 samples were obtained during the 90 minutes of emission scanning. Following centrifugation (10 min at 1,800 g), plasma was collected in 200 µL aliquots and activities were counted in a gamma counter (Wallac 1480 Wizard 3M Automatic Gamma Counter). Five samples (collected at 2, 16, 30, 50 and 70 min) were further processed by high-pressure liquid chromatography (HPLC) to measure the fraction of plasma activity representing unmetabolized parent compound. The unmetabolized parent fraction was fitted to a sum of 2 exponential functions with the smaller exponential rate constant constrained to the difference between the terminal washout rate of

the total plasma activity and the terminal washout rate of the cerebellum, as estimated from the data (S2). This curve was multiplied with the total plasma concentration to obtain an empirical parent compound curve. The empirical parent compound curve was then fitted to a sum of 3 exponentials (from the time of peak concentration) and this fitted curve was used as the input function for kinetic modeling. Peripheral clearance (L/hr) of unmetabolized radioligand was computed as the injected activity divided by the total area under the curve of the (decay-corrected) modeled plasma input function. Prior to radiotracer injection, a separate sample of arterial plasma was obtained and later spiked with radioligand to determine the free fraction (fraction not bound to plasma protein, f_p).

For each subject, a high-resolution structural MRI scan was acquired, and PET data were coregistered to the MRI scan. Regions of interest (ROIs) were drawn on the MRIs and transferred to the coregistered PET data. Extrastriatal ROIs included the orbital frontal cortex (Figure S1), anterior cingulate, medial prefrontal cortex, dorsal lateral prefrontal cortex, temporal cortex, parietal cortex, occipital cortex, parahippocampal gyrus, entorhinal cortex, insula, amygdala, genu, and uncus. A gray matter mask was applied to cortical ROIs so that only gray matter activity was measured in those regions (S3). Cerebellum (CER) was included as a reference region. All regions were defined as previously described (S3).

Data were analyzed by 2-tissue compartment modeling (2TC) with arterial plasma input using CER as a reference region. For 2TC modeling, total distribution volume (VT) was estimated in each brain region. CER VT was taken as an estimate of the nondisplaceable distribution volume (VND) and was also estimated by the 2TC model.

The outcome measures BPP and BPND were then determined from regional VT values according to the formulae:

Eq 1

$$BP_P = V_T(ROI) - V_T(CER) = \frac{f_P B_{avail}}{K_D}$$
$$BP_{ND} = \frac{V_T(ROI) - V_T(CER)}{V_T(CER)} = \frac{f_{ND} B_{avail}}{K_D}$$

where VT is total distribution volume, fP is the fraction of unmetabolized radioligand in plasma that is not protein bound, and fND is the fraction of free plus nonspecifically-bound radioligand in the brain.

KD is the equilibrium dissociation constant and BAVAIL is the concentration of 5-HT2A receptors

available for binding to [¹¹C]MDL100907 (S4). As can be seen, both measures are proportional to BAVAIL / KD, but with reference to different pools of free radioligand.

RESULTS

Scan Parameters

An overall mean difference was detected in injected mass [$F(2,51) = 3.06, p = .056$] with least-significant difference (LSD) post-hoc analyses indicating that the control group received greater mass than did both the PD-IED-IR patients with ($p = .043$) and without ($p = .050$) current physical aggression. Injected mass was not related to [^{11}C]MDL100907 BPND or BPP in the OFC across the total sample (BPND: $r = -.06, p = .683$; BPP: $r = -.16, p = .265$) or within any of the 3 diagnostic groups (BPND: $-.05 \leq r \leq .01, p \geq .86$; BPP: $-.15 \leq r \leq -.06, p \geq .58$ in all cases).

Peripheral clearance of [^{11}C]MDL100907 was significantly faster in the PD-IED-IR group without current physical aggression compared to the control group [overall $F(2,51) = 3.18, p = .050$; LSD post-hoc $p = .017$]. Clearance of [^{11}C]MDL100907 was quantitatively faster in PD-IED-IR patients without compared to patients with current physical aggression, with this difference reaching the level of a statistical trend ($p = .082$).

Regional Volumes

The mean ROI volumes by group are presented in Table S2. There were no group differences in the OFC or the other ROI volumes examined with the exception of the parietal cortex (PC) [overall $F(2,51) = 3.69, p = .032$]. Post-hoc LSD analyses indicated that the PC volumes of the PD-IED-IR patients with current physical aggression were significantly smaller than those of the control group ($p = .009$).

Examination of associations of demographic features with regional volumes across the sample indicated that age was significantly negatively related to the volumes of the DLPFC ($r = -.32, p = .017$) and MPFC ($r = -.35, p = .009$). Amygdala volumes were significantly greater in males ($M = 4261.47, SD = 962.87$) compared to females ($M = 3636.79, SD = 952.12$) [$t(52) = 2.22, p = .031$].

Associations of Clinical Measures with OFC [¹¹C]MDL100907 BPND and BPP

When adjusting for age and age-by-group, [¹¹C]MDL100907 OFC BPND was significantly associated with the Global Irritability subscale of the OAS-M ($r = .48, p = .009$); results were consistent when only age was included as a covariate ($r = .37, p = .048$). Similarly, when adjusting for age and age-by-group, OFC BPP was significantly associated with the Global Irritability subscale ($r = .43, p = .022$), and when only age was included as a covariate, a similar relationship, albeit at the level of a statistical trend, was observed ($r = .35, p = .064$).

DISCUSSION

An unanticipated finding was that of smaller parietal cortex volumes in patients with current physical aggression compared to healthy controls. It is not clear whether parietal cortex volume is related to impulsive aggression or a different symptom dimension. Our study was not optimally designed to assess volumetric differences, and the literature regarding the parietal cortex and impulsivity or aggression is sparse, at best. A small literature exists, however, implicating the parietal cortex in the dissociative (S5, S6), and psychotic-spectrum symptoms (S7) of BPD; this may be of relevance given the majority of our patients were diagnosed with BPD. We also observed greater amygdala volumes in males compared to females, which has been previously described in non-clinical populations (S8, S9).

Table S1. Patient Diagnostic Information

Age	Gender	Axis I Diagnoses	Axis II Diagnoses	IED-IR	Physical	Verbal
21	M	PTSD, SocPhb	BPD, ASPD, AvPD	Current	Current	Current
25	F	MDD(r)	BPD, OCPD	Current	Current	Current
28	F	MDD(r), PTSD(r), SpPhb, EtOH Dep(r), THC Ab(r)	BPD	Current	Current	Current
28	M	MDD(r), PTSD, EtOH Ab(r)	BPD, ASPD, PPD	Current	Current	Current
31	M	BDD	NPD, AvPD	Current	Current	Past
32	F	BP-II(r)	BPD, ASPD, PPD	Current	Current	Past
33	M	SocPhob, EtOH Ab(r), THC Ab(r)	BPD, NPD	Current	Current	Past
37	M	EtOH Ab(r)	BPD, NPD	Current	Current	Current
39	M	(none)	OCPD	Current	Current	Past
42	M	MDD(r), Dysth, GAD, EtOH Ab(r)	BPD	Current	Current	Current
46	M	MDD(r), GAD(r)	BPD, NPD, PPD, SPD	Current	Current	Current
48	M	MDD(r), SpPhb, EtOH Dep(r)	BPD, ASPD, PPD	Current	Current	Current
52	F	MDD(r), EtOH Dep(r), THC Ab(r), Stim Ab(r), PCP Ab(r)	BPD, PPD, SPD	Current	Current	Current
53	M	GAD	BPD, OCPD, PPD, SPD	Current	Current	Current
43	M	MDD(r), EtOH Dep(r), THC Dep(r)	BPD, NPD, ASPD, PPD	Current	Past	Current
28	M	MDD(r)	BPD	Current	Past	Current
35	M	MDD(r), EtOH Dep(r)	BPD, NPD, ASPD, PPD	Current	Past	Current
20	M	(none)	BPD, NPD, ASPD, DPD, PPD, SPD	Past	Past	Past
49	M	EtOH Dep(r)	SPD	Past	Past	Past
37	F	MDD(r), PSD(r) [EtOH, THC, Stim, Op, Coc, Sed Ab(r)]	BPD	Past	Past	Past
45	M	MDD(r), GAD, EtOH Dep(r), Coc Ab(r), PCP Ab(r)	BPD, NPD, ASPD, AvPD, OCPD, PPD, SPD	Past	Past	Past
36	M	Coc Ab(r)	ASPD	Past	Past	Past
51	M	(none)	NPD, ASPD, PPD, SPD	Past	Past	Past
30	F	MDD(r), OCD	BPD, NPD, OCPD, PPD, SPD	Past	Past	Past
37	M	MDD(r)	BPD, ASPD, OCPD, PPD	Current	No Hx	Current
21	M	THC Ab(r)	BPD	Current	No Hx	Current
30	F	MDD(r), GAD, OCD, SpPhb, BN(r)	BPD, AvPD, OCPD, PPD	Past	No Hx	Past
43	M	PTSD, EtOH Dep(r), THC Dep(r)	BPD, PPD	Past	No Hx	Past
39	M	MDD(r), PTSD	BPD, AvPD, PPD	Past	No Hx	Past

Note. Dark gray region = patients with current physical IED-IR; Medium gray region = patients with past physical IED-IR; Light gray region = patients with only verbal IED-IR

Ab, abuse; ASPD, antisocial personality disorder; AvPD, avoidant personality disorder; BDD, body dysmorphic disorder; BN, bulimia nervosa; BP-II, bipolar-II disorder; BPD, borderline personality disorder; Coc, cocaine; Dep, dependence; DPD, dependent personality disorder; Dysth, dysthymia; EtOH, alcohol; F, female; GAD, generalized anxiety disorder; Hx, history; IED-IR, intermittent explosive disorder-integrated research criteria; M, male; MDD, major depressive disorder; NPD, narcissistic personality disorder; OCD, obsessive-compulsive disorder; OCPD, obsessive-compulsive personality disorder; Op, opiate; PCP, phencyclidine; Physical, Physical IED-IR; PPD, paranoid personality disorder; PSD, polysubstance dependence; PTSD, post-traumatic stress disorder; (r), in remission; Sed, sedative; SocPhb, social phobia; SPD, schizotypal personality disorder; SpPhb, specific phobia; Stim, stimulant; THC, cannabis; Verbal, Verbal IED-IR

Table S2. Region of Interest (ROI) Volumes by Diagnostic Group

ROI (mm ³)	Current Physical IED-IR (n=14) ¹	Without Current Physical IED-IR (n=15) ²	Controls (n=25)	Group comparisons ³
OFC	12428.9 (3711.4)	13137.5 (6461.1)	13092.8 (4450.7)	<i>NS</i>
GEN	1011.2 (601.1)	1058.6 (281.1)	1319.6 (531.3)	<i>NS</i>
MPFC	6929.0 (3333.4)	8921.2 (3545.2)	9120.3 (3196.0)	<i>NS</i>
ACC	3878.9 (1661.4)	4001.9 (1543.8)	4328.2 (1437.2)	<i>NS</i>
TC	54614.6 (12468.5)	57979.2 (11163.2)	57811.1 (7656.4)	<i>NS</i>
DLPFC	28095.2 (7890.0)	32286.9 (8742.1)	34024.1 (7224.1)	<i>NS</i>
OC	43624.2 (8478.8)	51348.5 (13720.2)	45157.4 (9414.7)	<i>NS</i>
INS	6569.3 (1785.7)	7827.2 (1639.7)	7404.3 (1151.9)	<i>NS</i>
PC	52638.9 (14380.2)	60970.9 (15598.5)	65775.7 (13879.9)	Current Physical < Ctrl (p=.009)
ENT	2382.1 (1016.3)	3027.2 (601.2)	2623.1 (650.4)	<i>NS</i>
UNC	766.1 (292.7)	994.9 (542.4)	945.2 (469.9)	<i>NS</i>
PHG	7431.9 (1647.2)	7545.0 (1439.7)	8250.9 (1400.6)	<i>NS</i>
AMYG	3645.4 (1129.3)	4455.3 (848.2)	4065.4 (936.0)	<i>NS</i>

Note. Mean (standard deviation). Bolded data highlight the OFC, our *a priori* region of interest.

ACC, anterior cingulate cortex; AMYG, amygdala; DLPFC, dorsolateral prefrontal cortex; ENT, entorhinal cortex; GEN, genu; IED-IR, patients with intermittent explosive disorder-integrated research criteria; INS, insula; MPFC, medial prefrontal cortex; NS, nonsignificant; OC, occipital cortex; OFC, orbitofrontal cortex; PC, parietal cortex; PHG, parahippocampal gyrus; TC, temporal cortex; UNC, uncus

¹ Personality-disorder patients who met IED-IR with current physical aggression

² Personality-disorder patients who met IED-IR without current physical aggression

³ 3-group ANOVA conducted, followed by least-significance difference post-hoc tests when overall *F* significant.

Table S3. Comparison of [¹¹C]MDL100907 Binding Potential (BPND and BPP) and State Aggression Between IED-IR Patients with and without Histories of Past Alcohol/Substance Abuse and/or Dependence

Measure	IED-IR (+) Past Alcohol/Substance History (<i>n</i> =15) ¹ <i>M</i> (<i>SD</i>)	IED-IR (-) Past Alcohol/Substance History (<i>n</i> =14) ² <i>M</i> (<i>SD</i>)	Group comparisons ³
BPND	2.01 (.48)	2.41 (.81)	<i>p</i> = .219 ⁴
BPP	44.33 (12.29)	52.26 (16.98)	<i>p</i> = .265 ⁵
State Aggression: Assaultiveness ⁶	20.10 (16.12)	42.14 (88.01)	<i>p</i> = .694 ⁷
State Aggression: Global Irritability ⁸	4.97 (1.89)	5.29 (2.23)	<i>p</i> = .680 ⁹

Note. BPND and BPP are of [¹¹C]MDL100907 in the orbitofrontal cortex

IED-IR, intermittent explosive disorder-integrated research criteria; *M*, mean; *SD*, standard deviation

¹ Personality-disorder patients who met IED-IR with a history of past alcohol/substance abuse/dependence

² Personality-disorder patients who met IED-IR without a history of past alcohol/substance abuse/dependence

³ For BPND and BPP, 2-Group ANOVA (controlling for age) was performed; for Assaultiveness, Mann-Whitney test performed due to the non-normal distribution of scores (positive skew); for Global Irritability, *t*-test was employed.

⁴ $F(1,26) = 1.58$

⁵ $F(1,26) = 1.30$

⁶ Assaultiveness subscale of the Overt Aggression Scale-Modified (OAS-M)

⁷ Mann-Whitney $U = 96.0$

⁸ Global Irritability subscale of the OAS-M

⁹ $t(27) = .42$

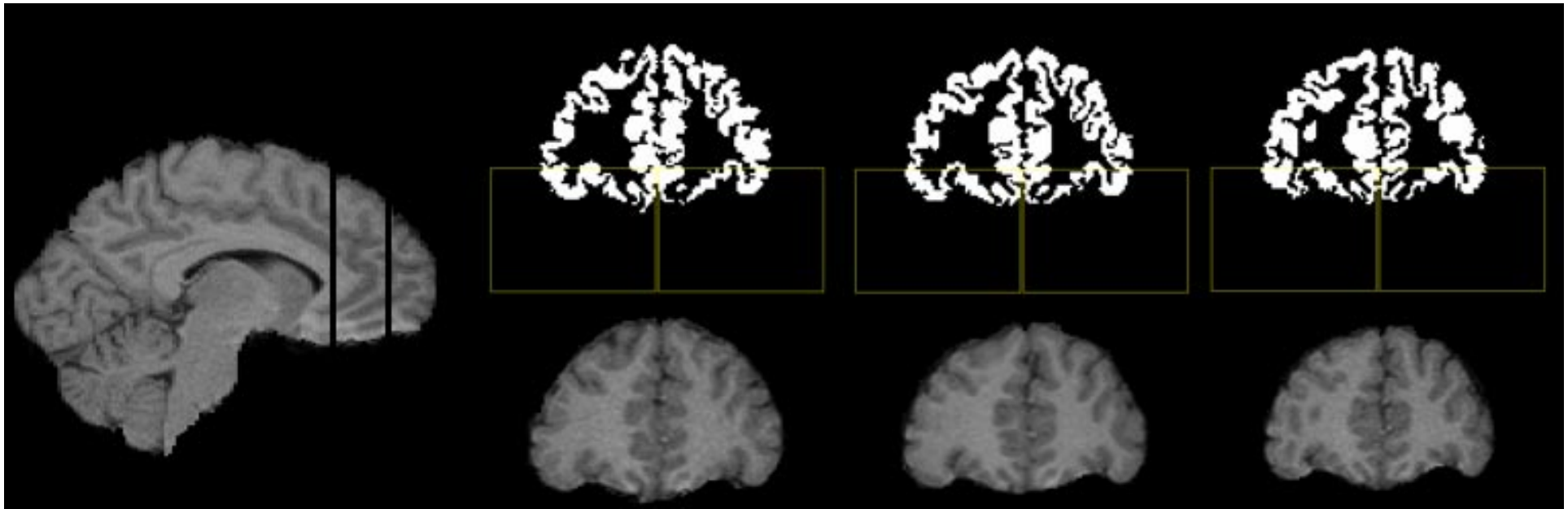


Figure S1. Derivation of the orbitofrontal cortex (OFC) region. Three representative coronal slices from the same subject, demonstrating how the OFC region is generated. The bottom row shows the MRI coronal slices, and the top row shows the gray matter mask with OFC boxes applied. PET data are sampled only from the gray matter voxels in the box. The black lines in the sagittal view (left) show the anterior and posterior boundaries of the region. The superior boundary of the box is the plane determined by the anterior and posterior commissures. The anterior boundary of the OFC is the first coronal slice on which both 1) the white matter tracts are connected (i.e., there are no detectable breaks in the white matter) and appear throughout the cortical gyri, and 2) the cortical gray matter strip is connected (i.e., there are no detectable breaks). The posterior boundary of the OFC is the coronal slice most immediately anterior to the point at which the corpus callosum is visible at the midline.

- S1. Lundkvist C, Halldin C, Ginovart N, Nyberg S, Swahn CG, Carr AA, *et al.* (1996): [11C]MDL 100907, a radioligand for selective imaging of 5-HT(2A) receptors with positron emission tomography. *Life Sci* 58:187-192.
- S2. Abi-Dargham A, Simpson N, Kegeles L, Parsey R, Hwang DR, Anjilvel S, *et al.* (1999): PET studies of binding competition between endogenous dopamine and the D1 radiotracer [11C]NNC 756. *Synapse* 32:93-109.
- S3. Abi-Dargham A, Martinez D, Mawlawi O, Simpson N, Hwang DR, Slifstein M, *et al.* (2000): Measurement of striatal and extrastriatal dopamine D-1 receptor binding potential with [C-11]NNC 112 in humans: Validation and reproducibility. *J Cerebr Blood F Met* 20:225-243.
- S4. Innis RB, Cunningham VJ, Delforge J, Fujita M, Gjedde A, Gunn RN, *et al.* (2007): Consensus nomenclature for in vivo imaging of reversibly binding radioligands. *J Cereb Blood Flow Metab* 27:1533-1539.
- S5. Irle E, Lange C, Weniger G, Sachsse U (2007): Size abnormalities of the superior parietal cortices are related to dissociation in borderline personality disorder. *Psychiatry Res* 156:139-149.
- S6. Lange C, Kracht L, Herholz K, Sachsse U, Irle E (2005): Reduced glucose metabolism in temporo-parietal cortices of women with borderline personality disorder. *Psychiatry Res* 139:115-126.
- S7. Irle E, Lange C, Sachsse U(2005): Reduced size and abnormal asymmetry of parietal cortex in women with borderline personality disorder. *Biol Psychiatry* 57:173-182.
- S8. Goldstein JM, Seidman LJ, Horton NJ, Makris N, Kennedy DN, Caviness VS Jr (2001): Normal sexual dimorphism of the adult human brain assessed by in vivo magnetic resonance imaging. *Cereb Cortex* 11:490-497.
- S9. Brierley B, Shaw P, David AS (2002): The human amygdala: a systematic review and meta-analysis of volumetric magnetic resonance imaging. *Brain Res Brain Res Rev* 39:84-105.